



## Review

# An overview of mathematical modeling of electrochemical supercapacitors/ultracapacitors



Innocent S. Ike <sup>a, b, \*</sup>, Iakovos Sigalas <sup>a</sup>, Sunny Iyuke <sup>a</sup>, Kenneth I. Ozoemena <sup>c</sup>

<sup>a</sup> School of Chemical and Metallurgical Engineering, University of the Witwatersrand, Johannesburg, South Africa

<sup>b</sup> Department of Chemical Engineering, Federal University of Technology, Owerri, Nigeria

<sup>c</sup> Energy Materials, Materials Science and Manufacturing, Council for Scientific and Industrial Research (CSIR), Pretoria, South Africa

## HIGHLIGHTS

- The review presents an overview of the benefits and drawbacks of the existing models and future directions.
- Synergy between existing models to realizing a real-life model was articulated.
- Parameters to be captured in theoretical basis for designs of various types of ESs were proposed.
- It surveyed the up to date advances on key parameters such as temperature distributions, mechanisms of self-discharge, etc.

## ARTICLE INFO

### Article history:

Received 4 May 2014

Received in revised form

11 August 2014

Accepted 9 September 2014

Available online

### Keywords:

Electric double layer

Charge and discharge

Electrodes

Conductivity and electrolyte

## ABSTRACT

Varieties of electrochemical supercapacitors ESs models has been presented in the literature, but most do not capture all necessary parameters to build theoretical basis for calculations and optimization of parameters of various types and designs of ESs with simultaneous account of properties of electrode materials, electrolytes, separators, designs, and values of charge and discharge currents of the ES. This work reviews existing models and discusses the benefits and setbacks of each type and attempt to synergize the existing models to realize more real-life model built on realistic assumptions and with thermal model (temperature distribution) that is useful for thermal management/cooling strategies for supercapacitors cell.

Results in literature generally show the basic relationship between supercapacitors components, but hardly any existing model is currently able to take due account of ESs parameters and other factors like internal temperature rise and interfacial electric field in a rigorous manner, hence the discrepancy between results of theoretical and experimental measurements of parameters of real-life supercapacitors.

In order to build supercapacitors with improved key parameters and optimal design, account of thickness, strong dependence of capacitance of polarizable electrodes on their potential, temperature distributions, specific mechanisms or combination of different mechanisms of self-discharge, type and value of conductivity of electrodes material and conductivity of electrolyte in its pores must be considered.

© 2014 Elsevier B.V. All rights reserved.

## 1. Introduction

Electrochemical supercapacitors ESs that store charges through electrostatic charging of a double layer and also through a Faradaic reaction have higher energy density than conventional electrostatic

capacitors as well as higher power density than batteries in general. Owing to their promises as electrical energy storage devices, ESs has been the subject of intense studies in recent years. Electric double layer supercapacitors EDLSs store electric charges electrostatically using reversible adsorption of ions of the electrolyte onto active electrode materials that are electrochemically stable and have high accessible specific surface area SSA, forming the electric double layer at electrode/electrolyte interfaces accessible to ions present in the electrolyte [1–5]. The advantages of EDLSs are high power density, long lifecycle, high efficiency, and wide range of

\* Corresponding author. School of Chemical and Metallurgical Engineering, University of the Witwatersrand, Johannesburg, South Africa.

E-mail addresses: [hephzibethel@yahoo.co.uk](mailto:hephzibethel@yahoo.co.uk), [innocent.ike@students.wits.ac.za](mailto:innocent.ike@students.wits.ac.za) (I.S. Ike).

operating temperatures, environmental friendliness, and safety. EDLSs serve as a bridging function for the power/energy gap of convectional dielectric capacitors [6].

Recently, ES is gaining more attention due to the practical potential in applications areas with increasing power demands. Because of reversible electrochemical energy storage the supercapacitors can be recharged very quickly with best long cycle life. Energy storage is by means of static charge rather than of an electro-chemical process (inherent to common battery) [7]. ESs store the energy via two operating mechanisms: (i) electric double-layer capacitance (EDLC) [5,8] which results from the electrical double-layer surrounding the surface of electrode, that is, the depletion of the oppositely charged species which stores the energy at the interface of the electrode and the electrolyte, respectively. The accumulation of electrons at the electrode is a non-Faradaic process. The specific capacitance of an EDLS is measured/determined by an expression:

$$C = \frac{\epsilon_r \epsilon_0 A}{d} \quad (1)$$

where  $\epsilon_r$  is the relative permittivity of the medium in the electrical double-layer,  $\epsilon_0$  is the permittivity of vacuum,  $A$  is the specific surface area of the electrode, and  $d$  is the effective thickness of the electrical double-layer. (ii) Pseudo-capacitance, which is originated from the redox reaction of the electrode material with the electrolyte [9–11]. The accumulation of electrons at the electrode is a Faradaic process where the electrons produced by the redox reaction are transferred across the electrolyte-electrode interface. The theoretical pseudo-capacitance of metal oxide can be expressed as:

$$C = \frac{nF}{MV} \quad (2)$$

where  $n$  is the mean number of the electrons transferred in the redox reaction,  $F$  is the Faraday constant,  $M$  is the molar mass of the metal oxide and  $V$  is the operating voltage window. The energy density ( $E$ ) of a supercapacitor is expressed as

$$E = \frac{CV^2}{2} \quad (3)$$

The maximum power density of a supercapacitor is determined by

$$P_{MAX} = \frac{V^2}{4R} \quad (4)$$

where  $R$  is the equivalent series resistance of all the components in the device. EDLC and pseudo-capacitance can simultaneously be generated in a single supercapacitor to form a hybrid supercapacitor. Hybrid supercapacitor can achieve higher energy and power densities while keeping good cycling stability by utilizing both faradaic and non-faradaic processes simultaneously to store charges. Other types of hybrid supercapacitors are battery-like hybrids and composite hybrids. Various types of supercapacitors combining different electrode materials in order to improve the device performance have been developed in practice.

The key performance parameters of supercapacitors are specific capacitance (normalized by electrode mass, volume, or area), energy density, power density, rate capability (retained capacitance at a high current loading) and cycling stability [12]. To increase the energy and power densities of a supercapacitor, it is desirable to increase the specific capacitance ( $C$ ) and the operating voltage window ( $V$ ) and also reduce the equivalent series resistance ( $R$ ). The maximum operating voltage window ( $V_m$ ) for supercapacitor is

mainly dependent on the electrolyte used, which is limited by the stability of the electrolyte. For the supercapacitors based on the aqueous electrolyte, the  $V_m$  is 1 V. One of the current research trends in supercapacitors is to develop non-aqueous electrolytes with high  $V_m$ . For a larger double-layer capacitance it would be necessary to produce a thin, high surface-area EDL with a combination of high surface area (about  $200 \text{ m}^2 \text{ g}^{-1}$ ) and extremely small charge separation ( $\delta \sim 10 \text{ \AA}$ ) [9].

Regular double-layer capacitance generates from the potential-dependence of the surface density of charges stored electrostatically at the interfaces of the supercapacitors electrodes as indicated by Conway [9]. An illustration of the basic components and design of an EDLS and the movement of cations and anions in the cell is shown in Fig. 1 above. A double-layer supercapacitors device must employ two double layers, one at each electrode interface, one working against the other on charge or discharge, as emphasized by Conway [9] and shown diagrammatically in Fig. 2(a) below. Pseudocapacitance generates in some electrosorption processes and in redox reactions at electrode surfaces or oxide films, and is faradaic in origin involving the passage of charge across the double layer.

Contrary to the EDLSs, the pseudo-capacitors store energy through faradaic process, involving fast and reversible redox reactions between electrolyte and electro-active materials on the electrode surface [5], see Fig. 2(b) below. Pseudocapacitors can achieve much higher pseudo-capacitance than the EDL capacitance. Notwithstanding, further real-life applications of these electro-active materials to pseudo-capacitors are still restricted by low power density that arises from the poor electrical conductivity that restricts fast electron transport and by the lack of pure cycling stability due to the easily damaged structure of the materials during redox process. Hybrid supercapacitors can achieve higher energy and power densities while keeping good cycling stability by utilizing both faradaic and non-faradaic processes simultaneously to store charges as shown in Fig. 2(c) below. Other types of hybrid supercapacitors are battery-like hybrids and composite hybrids. Various types of supercapacitors combining different electrode materials in order to improve the device performance have been developed in practice.

Supercapacitors consist of two activated carbon electrodes immersed into an ionic electrolyte. The two electrodes are separated by a membrane, separator which allows the mobility of the charged ions but prevents electric contact as shown in Fig. 1 above. The requirements for the separators are electrochemical stability (high purity and electrochemical stability of the materials), high porosity, high thermal inertia, and chemical inertia versus electrolyte. Furthermore, because a separator is non-active in a supercapacitor, the separator thickness should be as thin as possible and the cost must be relatively low. Its minimum size nevertheless is constrained by the following: 1) the electrical shortening failure risk owing to free carbon particles, which may create a contact between the electrodes (high self-discharge rate or short circuit) [13]. 2) the mechanical strength in order allows the winding process.

The electrode thickness and internal area, the porosities and particle sizes of the active material, as well as the materials selected for the electrolyte and electrode are the design elements that can be more accurately investigated with microstructural models such as that described by Verbrugge and Liub [15]. ESs when in use encounter “self-heating,” which is accelerated as the interfacial electric field (related to voltage across the device) and temperature (related to self-heating/internal power dissipated that can be correlated with the current profile) increase. The self-heating process raises the temperature of the device by promoting irreversible side reactions which decrease the ionic conductivity of the electrolyte. The decrease in the ionic conductivity, assuming all

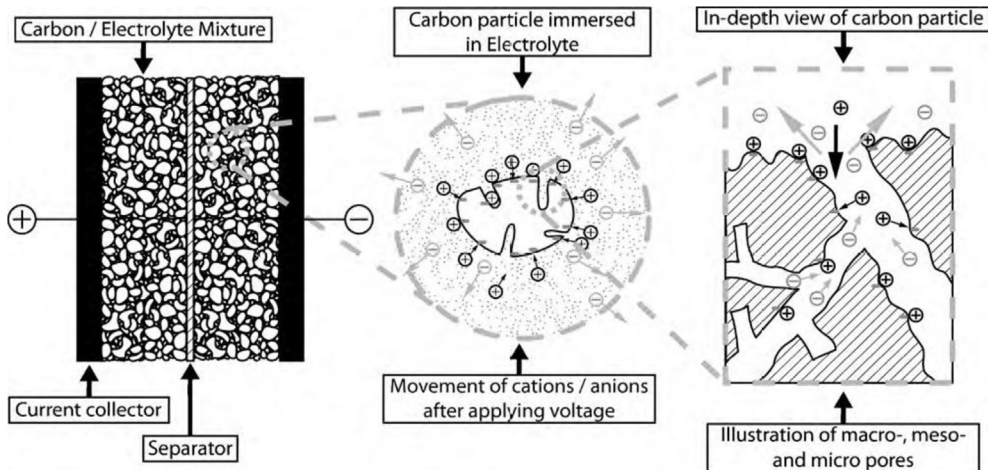


**Fig. 1.** Illustration of the basic components and design of an EDLS. Arrows indicate the direction of movement for the cations and anions [75].

other things remain equal, results in additional heat generation which over time leads to thermal runaway.

Mathematical modelling and numerical simulations of electrochemical energy systems like batteries and supercapacitors play a vital role in their design and estimation of performance. However, deriving and solving these models analytically and numerically is a challenging task for two main reasons: first, a model that intends to capture all physical and chemical phenomena has to consider conservation of charge, species and energy along with the necessary constitutive relations for the double-layer charging and faradaic reaction; and second, it has to do same for all the functional layers and groups within the cell at differing length scales (macroscale and microscale) [16]. The theoretical research and

modelling of various processes which take place in the supercapacitors are of great scientific interest and as well as the basis for understanding the parameters and the practical proposals targeted at building supercapacitors with improved energy and power parameters. Besides, the bulk of the research on supercapacitors and their components are experimental works. The quite reliable experimental results on ground and their increasing number have initiated necessary prerequisites for the development of a modern theory of ESs, which will enhance the development of ESs with parameters that meet modern requirements and launch them in mass commercial production [17].

Characteristics and parameters of the processes occurring in ESs are closely interrelated and are dependent on the physical,

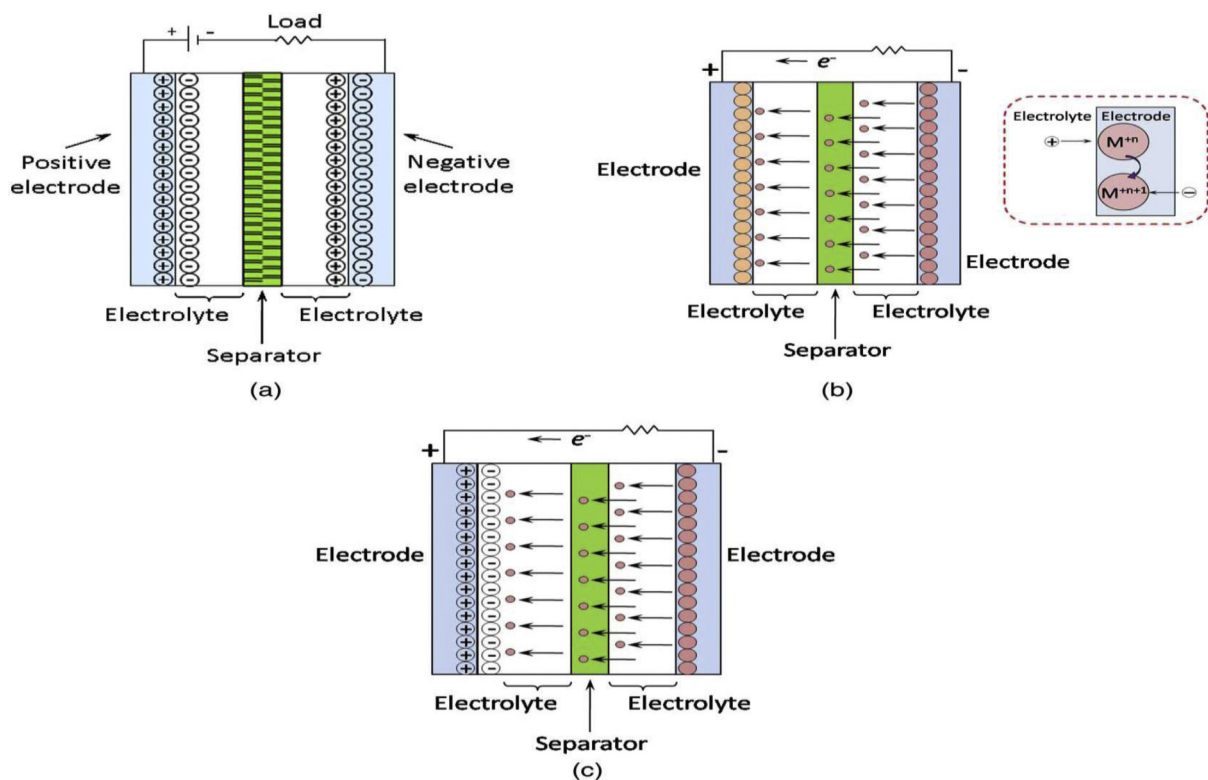


**Fig. 2.** Schematic representation of supercapacitor's types: (a) EDLS type; (b) pseudocapacitor type; (c) hybrid capacitor type (the figure is not to scale) [14].

electrical, electrochemical and crystallographic parameters of electrodes and electrolyte materials, and the design of its components and supercapacitor as a whole. Therefore, the modelling of supercapacitor for the determination of its energy, capacity, and other operation characteristics is inconceivable without proper account of its component parameters. The bulk of the researchers do not consider the physical, electrical, and structural properties of their electrode materials and components while modelling and estimating the supercapacitor's parameters hence the discrepancy between the results of theoretical and experimental measurements of the parameters of real-life supercapacitors [17]. Most of the existing models assume that the energy is stored purely by electric double layer at the electrode interface and neglects the electrochemical side reactions at the interface [18]. On the other hand, models that account for these electrochemical side reactions [19–21] oversimplify the reaction dynamics by not considering temperature coupling. Furthermore, the effect of pores and varying pore size has been only treated in a semi-qualitative manner and there is no single model that takes all the factors into account in a rigorous manner. Hence, it is important to recognise the setbacks in the existing modelling approaches, which are mostly not based on first principles, and then develop a first principles approach to compensate for the modelling gaps.

A first principles model should be able to predict in real time the internal temperature and interfacial electric field for the following reasons: 1) to facilitate more accurate lifetime predictions. 2) to facilitate the process of sizing the ESs along with other parallelled storage devices if the objective is to maintain a bus voltage within certain limits for arbitrary loading profiles or to increase battery lifetime, and 3) to guide the development of porous structures (materials and geometries) that allow stored energy to be extracted at faster rates [1]. Existing models for all energy storage devices ESs inclusive are currently not able to accurately predict the internal temperature rise, interfacial electric field, and the temporal voltage response for arbitrary charge–discharge current profiles.

In this review, we considered progress made so far in the field of modelling and simulation of supercapacitors by looking at two basic kinds of supercapacitors and their hybrid supercapacitors. We discussed their mechanisms with an aim to explore their effective ways to achieve high supercapacitor performance. The existing models of ESs were reviewed and the benefits and drawbacks of each type discussed with the view to exploit the relative advantages and appraise the relative disadvantages of models to realize synergic and more realistic models incorporating a thermal model that account for temperature distribution inside a cylindrical and rectangular structured supercapacitor cell.

The main objectives are to develop a mathematical description of characteristics of symmetric and asymmetric ESs and parameters of the processes therein subject to the physical, electrical, electrochemical and crystallographic parameters of electrode materials, electrolyte, and the design of the components and the supercapacitor as a whole; to build a theoretical basis for the calculations and improvement of the parameters of various types and designs of symmetric and asymmetric ESs with simultaneous account of properties of electrode materials, designs, and spatial structures of electrodes and separator; to provide an ideal alternative to the time-consuming task of numerous experiments by providing guidelines for the design and the optimization methodology for ES cell for a wide range of applications using a modelling approach; to optimize the parameters of the supercapacitors subject to the type and value of conductivity of the electrodes, thickness, porosity and specific capacitance of electrodes, conductivity of electrolyte, thickness and porosity of separator and the values of charge and discharge currents of the ES.

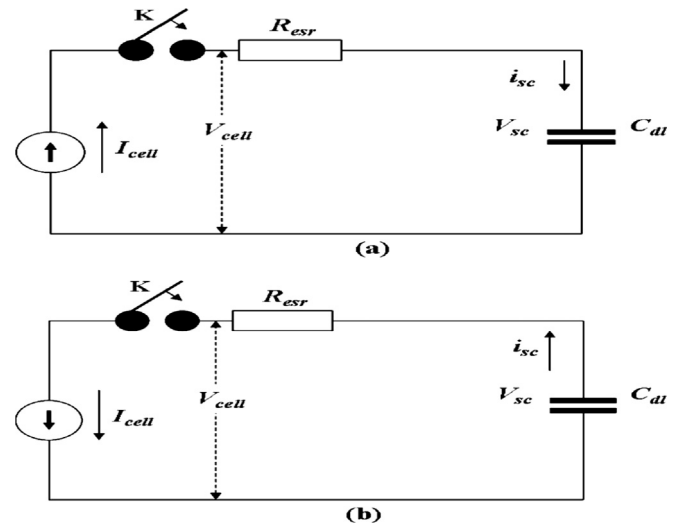


**Fig. 3.** Proposed equivalent circuits of a double-layer supercapacitor at a constant current charging (a) and discharging (b) in the absence of both parallel leakage process and electrochemical decomposition of the solvent.  $K$ : electric switcher;  $R_{esr}$ : equivalent series resistance;  $I_{cell}$ : constant current for charging or discharging the supercapacitor;  $V_{cell}$ : supercapacitor cell voltage;  $C_{dl}$ : double-layer capacitance;  $V_{sc}$ : voltage across the  $C_{dl}$ ; and  $i_{sc}$ : current used to charge or discharge  $C_{dl}$ ; respectively [6].

## 2. Current status of electrochemical supercapacitors modelling

Theoretical models for electrochemical supercapacitors range from the original Helmholtz model and mean-field continuum models, the surface curvature-based post-Helmholtz models and the modern atomistic simulations. Realistic models of supercapacitors can be built using the high level of development of classical and quantum molecular dynamics methods as well as the parallel high performance computing.

These classes of models for an electrochemical supercapacitor have been proposed by authors/researchers: empirical, dissipative transmission line, continuum models (Poisson–Nernst–Planck equations), atomistic models (Monte Carlo, molecular dynamics), Quantum models (ab initio quantum chemistry and Density Functional Theory, DFT) and simplified analytical models. Each approach has been developed for a different purpose and, thus, exhibits different advantages and limitations.

### 2.1. Empirical models

This empirical electrical equivalent circuit model is often referred to as a three-branch model and assumes that the immediate branch capacitance is voltage dependent and the long-term branch only accounts for a variation in charge for 30 min at the most. One of the first empirical models that addressed the variation of capacitance (or the rate of change of terminal voltage) as a function of time was developed by Zubietra and Bonert [22].

Empirical models provide a much better estimate of the ES's electrical characteristics than a simple  $RC$  circuit and also it allows the users to easily incorporate the model into their system simulations. In addition, empirical models could be used to characterize parameters such as self-discharge and leakage current [23].

Shuai et al. [6] presented some simple mathematical models incorporating the voltage-independent parallel leakage process and electrochemical decomposition to describe the supercapacitors charge and discharge behaviours in order to give a fundamental understanding of supercapacitors charging and discharging behaviours through experiment validation. Experiment data were

simulated to obtain the desired values of parameters such as specific capacitance and equivalent series resistance from which both the energy and power density can be calculated using the models. The simulated parameter values considering both parallel leakages and solvent decomposition could be used to predict supercapacitor's self-discharge and shelf-life, performance/efficiency losses, as well as the limiting workable cell voltage of the supercapacitors. These models are therefore useful in evaluating and diagnosing the supercapacitors cells and as well is a tool for understanding charging-discharging behaviour of the supercapacitors. Also, the models could as well be useful in obtaining the essential parameters of the supercapacitors such as equivalent series resistance and capacitance based on the recorded curves of charging–discharging.

Fig. 3 shows an electrical equivalent circuit of a double layer supercapacitors that is charged/discharged at a constant cell current in the absent of both parallel leakage and electrochemical decomposition of solvent. The current used to charge or discharge the double layer capacitance ( $i_{sc}$ ) is equal to the charging current ( $I_{cell}$ ), which has a constant value given by Equation (5) assuming that before the charging starts, the supercapacitor is at zero-charge state, that is, the voltage across the supercapacitor ( $V_{sc}$ ) is equal to zero.

$$I_{cell} = i_{sc} \quad (5)$$

The voltage across the supercapacitor when the charge process is then started as a result of turning on the switch can be expressed as Equation (6) below.

$$V_{sc} = \frac{1}{C_{dl}} \int_{t=0}^{t=t} i_{sc} dt = \frac{1}{C_{dl}} \int_{t=0}^{t=t} I_{cell} dt = \frac{I_{cell}}{C_{dl}} t \quad (6)$$

The supercapacitors cell voltage during charging process can therefore be expressed as Equation (7) below.

$$V_{cell} = I_{cell} R_{esr} + V_{sc} = I_{cell} R_{esr} + \frac{I_{cell}}{C_{dl}} t \quad (7)$$

If the supercapacitors are charged to a designed cell voltage of  $V_{cell}^{\max}$ , a discharge process at a constant current ( $I_{cell}$ ) can be started immediately, as shown in Fig. 3(b). Notice that at this desired cell voltage (or maximum cell voltage) of  $V_{cell}^{\max}$ , the voltage across the double layer capacitance ( $C_{dl}$ ),  $V_{sc}^0$ , should be given by Equation (8) and in the instance of discharging, this  $V_{sc}^0$  will be the load to discharge the supercapacitors and the cell voltage ( $V_{cell}$ ) during discharging process can be expressed as Equation (9) shown below.

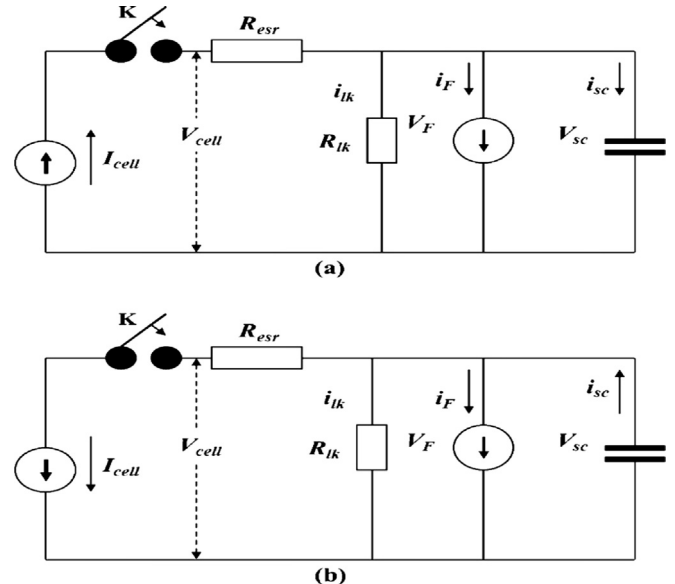


Fig. 4. Proposed equivalent circuits for a double-layer supercapacitor at a constant current charging (a) and discharging (b) in the presence of electrochemical decomposition of the solvent.  $K$ : electric switcher;  $R_{esr}$ : equivalent series resistance;  $R_{lk}$ : parallel leakage resistance;  $i_{lk}$ : parallel leakage current;  $I_{cell}$ : constant current for charging or discharging;  $V_{cell}$ : supercapacitor cell voltage;  $i_F$ : current of solvent electrochemical decomposition;  $C_{dl}$ : double-layer capacitance;  $i_{sc}$ : current used to charge or discharge the double-layer capacitance;  $V_F$ : electrode potential of the solvent electrochemical decomposition; and  $V_{sc}$  ( $=V_F$ ): voltage across the double-layer capacitance, respectively [6].

$$V_{sc}^0 = V_{cell}^{\max} - I_{cell} R_{esr} \quad (8)$$

$$V_{cell} = V_{sc}^0 - I_{cell} R_{esr} - \frac{I_{cell}}{C_{dl}} t \quad (9)$$

Parameters like the double-layer capacitance ( $C_{dl}$ ), the voltage across the double layer capacitance at the end of charging ( $V_{sc}^0$ ), as well as equivalent series resistance ( $R_{esr}$ ) with the aids of both the charge and discharge curves, can be simulated from Equations (8) and (9), respectively. Fig. 4 shows the electrical equivalent circuit of a double layer supercapacitor for constant current charging/discharging in the presence of both parallel leakage process and electrochemical decomposition of the solvent. A constant charging current ( $I_{cell}$ ) integration equation for the charge and discharge processes can be written as Equations (10) and (11) respectively.

$$i_{sc} + \exp\left(\frac{-\Delta V^0}{b_p + b_n}\right) \exp\left(\frac{1}{(b_p + b_n)C_{dl}} \int_{t=0}^{t=t} i_{sc} dt\right) + \frac{1}{R_{lk} C_{dl}} \int_{t=0}^{t=t} i_{sc} dt - I_{cell} = 0 \quad (10)$$

$$i_{sc} - \exp\left(\frac{V_{sc}^0 - \Delta V^0}{b_p + b_n}\right) \exp\left(-\frac{1}{(b_p + b_n)C_{dl}} \int_{t=0}^{t=t} i_{sc} dt\right) - \frac{1}{R_{lk} C_{dl}} \int_{t=0}^{t=t} i_{sc} dt - I_{cell} = 0 \quad (11)$$

The cell voltages ( $V_{\text{cell}}$ ) for the charge and discharge process in this Fig. 4 are expressed respectively as Equations (12) and (13) shown below.

$$V_{\text{cell}} = I_{\text{cell}} R_{\text{Esr}} + V_{\text{SC}} = I_{\text{cell}} R_{\text{Esr}} + \frac{1}{C_{\text{dl}}} \int_{t=0}^{t=t} i_{\text{SC}} dt \quad (12)$$

$$V_{\text{cell}} = -I_{\text{cell}} R_{\text{Esr}} + V_{\text{SC}} = V_{\text{SC}}^0 - I_{\text{cell}} R_{\text{Esr}} - \frac{1}{C_{\text{dl}}} \int_{t=0}^{t=t} i_{\text{SC}} dt \quad (13)$$

The models developed could be used to describe the charge and discharge behaviours of supercapacitors in the presence of both voltage-independent parallel leakage process and solvent decomposition as suggested by its ability to reasonably fit the experiment data. However, there is a slightly mismatch/difference that might have originated from experimental trivial factors such the effect of gaseous evolution, dissolution of current collectors, electrolyte crystallization in separator, assembly quality, and etc. at the discharge curves in particular.

The main setbacks of these models are the decreased accuracy of the model for 1) the operating conditions (i.e., initial voltage level, loading profile, etc.) that differ from those used for parameter extraction [24], and 2) longer time intervals where the internally generated heat changes the electrical characteristics of the supercapacitor. Because the models were not derived from fundamental basis of physics of the supercapacitor, they are incapable of estimating the internal temperature rise and thus, are only accurate if the temperature rise is inconsequential. On this understanding, the models cannot be used to predict the lifetime of a particular supercapacitor.

## 2.2. Dissipation transmission line models

The porous structure of the electrodes that impedes the movement of ions to interfacial sites located deep within a pore is one of the main reasons for the nonlinear rise of terminal voltage is. It is, thus, desirable to have a model that describes the transient and steady-state response of the porous electrolyte region since the bulk electrolyte region can be modelled to first order by a simple resistor. The first porous electrode model, developed by de Levie [25], treated the double-layer interfacial capacitance along a porous electrode's wall as a dissipative transmission line, a distributed double-layer capacitance and a distributed electrolyte resistance. The model assumes a straight, cylindrical pore of uniform diameter and a perfectly conducting electrode as presented in Fig. 5 below.

The effect of ion depletion on the charging rate of porous electrodes deserves further scrutiny for several reasons; 1) it will improve understanding of performance limits of double-layer

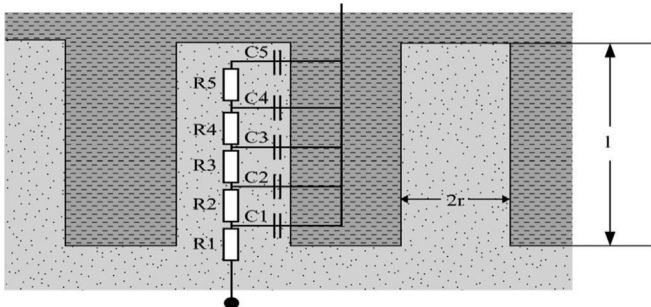


Fig. 5. Transmission line equivalent electrical circuit model [22].

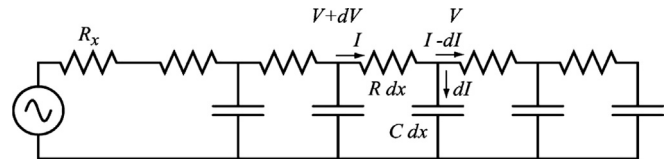


Fig. 6. De Levie's transmission line equivalent circuit for an electrolyte filled conducting pore [129].

supercapacitors as a function of device parameters. For instance, depletion can occur in both the electrodes and the separator, and tuning geometry may improve power and linearity.

- 2) the study of this phenomenon raises fundamental questions about the relationship between the adsorption and transport of ions in nanoporous conductors and about the influence of differing ion mobilities on these effects.

The de Levie model treats the pore as a distributed RC circuit Fig. 6 and states that voltage and current vary with respect to time  $t$  and position  $x$  along the pore through the following differential Equations (14) and (15).

$$\frac{dV}{dx} = -IR \quad (14)$$

$$\frac{dI}{dx} = -C \frac{dV}{dt} \quad (15)$$

where  $C$  and  $R$  are capacitance per unit length and resistance per unit length, respectively. De Levie assumed that the concentration (and therefore solution resistance) throughout the entire pore is constant.

Basically the available capacitance is maximal at low frequency, as could be explained with the longer time available for the ions in the electrolyte to get to the surface which is located deep in the carbon pores. Only the superficial carbon surface is accessible for the ions at higher frequency, hence much smaller capacitance.

The series resistance is composed of an electronic and an ionic part, the electronic contribution comes from the ohmic resistance in the conductor and in the carbon particles while the ionic contribution comes from the ions mobility in the electrolyte.

Conclusively, the current and energy for a given voltage are quite larger than what were expected on the base of the classical expressions in the instance of constant capacitance.

The value of capacitance and the series resistance varies over the frequency spectrum and the performance may be determined with an Impedance Spectrum analyzer [130]. To account for the voltage, temperature and frequency dependences, a simple equivalent electrical circuit has been developed by Rafik et al. [23] using a combination of the De Levie frequency model and Zubieta voltage model with the addition of a function to take into account the temperature dependence.

The main advantage of the dissipative transmission line model is its capability to provide a direct linkage between pore structures and the time response, which has been well accepted by the researchers in the field of ESs. It also provides a first-order estimate of the exponential rise/decay of the voltage level with the assumption of a constant current charge/discharge cycle, and is based on the physical structure of the interface instead of attempting to match the experimental measurements through right choice of passive circuit element combinations. However, this approach considers only limited aspects of interfacial dynamics (i.e., assuming a homogeneous electrolyte with a constant resistance throughout the

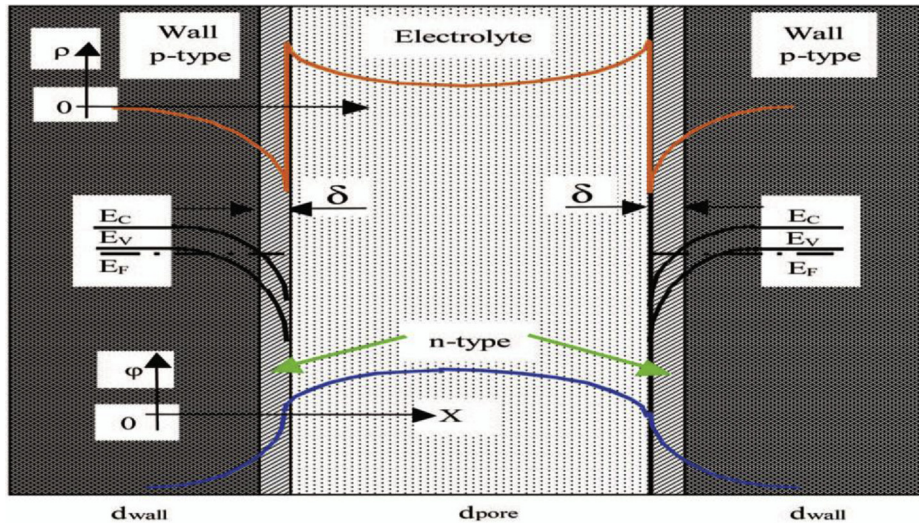


**Fig. 7.** Distributions of electric charge and potentials in the walls of cylindrical shaped pores and in the electrolyte which is inside the pores of the negative electrode with p-type conductivity [17].

pore, neglecting the temperature dependence of the parameters, etc.) and is mainly used for particular purposes such as electrodes synthesis improvement [26], study of self-discharge behaviour [27], and prediction of surface impedance of the electrode [28].

### 2.3. Continuum models (Poisson-Nernst-Planck equations)

The most exact modelling approach currently available exploited the Poisson–Nernst–Planck (PNP) electrodiffusion theory to represent the electrode–electrolyte interface but the physicochemical parameters was made functions of their local surroundings as opposed to a constant value since the electric field at the interface is large. The PNP theory predicts the properties of bulk electrolyte accurately when the physicochemical parameters are held constant. Helmholtz [29] proposed an EDL model which consists of a simple separation of charges at electrode/electrolyte interface similar to a convectional parallel-plate capacitor to determine the specific area capacitance independent of surface potential and electrolyte concentration though that was not observed experimentally [30]. The Helmholtz model was modified by Gouy [30] and Chapman [31] with the consideration of the fact that ion concentration should be continuous in electrolyte solution which resulted to Gouy–Chapman model. This model includes the effects of both the electrode potential and the bulk ionic concentration on the local ionic concentration and potential field in the electrolyte utilizing Boltzmann distribution function [29]. Chapman [31] derived and solved the steady-state Poisson–Boltzmann equation to predict electric potential in the diffuse layer. However, even for very dilute solutions, this theory predicts unrealistically large ion concentrations for surface potentials of just a fraction of 1 V. This could be as a result of the fact that the ions are assumed to be point charges, but in reality they have a finite size [32]. Therefore, this theory cannot be used to model actual EDLs with a typical surface potential of 1 V and bulk electrolyte concentration of 1 mol L<sup>-1</sup>.

Stern combined the Helmholtz and Gouy–Chapman models to explicitly describe the ion concentration in two distinct regions namely: (1) the inner region near the electrode called the Stern layer, and (2) the outer region called the diffuse layer [33]. Grahame [34] improved Stern's model by considering that in the Stern layer, adsorption of anions and cations at the electrode surface lead to different double layer thicknesses [9]. The model developed by

Stern [33] and Grahame [34] is usually referred to as the Stern model [35].

Hainan Wang and Laurent Pilon developed a three-dimensional (3D) model based on continuum theory for simulating EDLs with ordered mesoporous electrode structures and simultaneously and rigorously accounted for (1) 3D electrode morphology, (2) finite ion size, (3) Stern and diffuse layers, and (4) the dependency of the electrolyte dielectric permittivity on the local electric field [36]. They derived a new set of boundary conditions to account for the Stern layer without simulating it in the electrolyte domain. The model was then used to simulate faithfully the electrode morphology of CP204-S15 mesoporous carbon EDLs synthesized and characterized by Woo et al. [37].

This made possible the simulations of EDLs with 3D ordered electrode structures while simultaneously and accurately accounting for (i) the Stern and diffuse layers, (ii) finite ion size, and (iii) the dependency of electrolyte permittivity on the local electric field [36].

### 2.4. Atomistic models (Monte Carlos, molecular dynamics)

Classical and quantum molecular dynamics simulations can provide the most accurate description of the electric double layer.

The state of the development of classical and quantum molecular dynamics and use of parallel high performance calculations permit the construction of realistic models of such systems. The consistent classical consideration of the electric double layer at the interface between a metal and ionic liquid was performed in Ref. [49]. The molecular dynamics simulation of solid electrolytes with carbon nanotubes was carried out by Chaban [50] and [51]. Such a classical model makes it possible to satisfactorily describe the ionic subsystem of the electrolyte, but does not provide information on electron subsystem of the material of the electron–hole conductor of the electrode.

Molecular dynamics (MD) simulation provides the most fundamental and flexible ground for analysis of molecular interactions. This has been used extensively in modelling of electroosmotic flow (EOF) [38–43] and to treat the higher charge densities of importance in EDL supercapacitors [44–46].

However, this entail considerable computational cost hence made it impractical for treating time and length scales found in many applications. Challenges also arise in applying boundary

conditions and computing long-range Coulombic interactions. For these reasons, alternative methods are still needed.

Using the results of quantum molecular dynamics calculations of Lankin et al. [47], the maximum specific capacity of electric double layer EDL on the surface of the electrode made of pure defect-free graphite has been estimated and the estimation is in good agreement with the existing experimental data. The description of the dense part of the electric double layer is complicated because the distributions of the potentials in it cannot be described by the averaged charge densities [48]. In this case, correlations between the positions of charged particles should be taken into consideration. Due to this reason, the development of a consistent model of the dense part of the EDL is difficult.

Molecular modelling can provide an atomistic level understanding of the equilibrium and dynamic phenomena occurring in an EDLs. The accuracy of molecular modelling depends largely on the validity of the force fields used in describing the molecular interactions in the fluid phase and the geometry and force fields of the model electrode. Monte Carlo (MC) and molecular dynamics (MD) are the most favoured molecular simulation techniques available. Molecular Dynamics investigations of temperature influence on capacitance showed a positive capacitance dependence on temperature for OLC-based supercapacitors and a weak dependence of capacitance on temperature for CNT-based supercapacitors, in line with experimental observations. Molecular insights into RTIL-based supercapacitors, reviewed in this perspective could facilitate the design and development of a new generation of energy storage devices and supercapacitors in particular.

On the basis of mean-field theory and Monte Carlos (MC) simulations, Kondrat et al. [91,92] attributed the increase of capacitance to the “superionic state” of ions inside pores. Molecular dynamics (MD) simulations have reproduced the capacitance-voltage trend measured in experiments with both solvent electrolytes and RTILs considering the van der Waals interactions and complex ionic structure [93,94].

Also a DFT study showed a bell-shaped curve due to the co-ion removal of counter-ion and counter-ion addition with an absence of capacitance increase [95]. This observation in DFT calculations is probably as a result of the simplified RTIL ions in the restricted primitive model as well as the selected pore size.

Huang et al. [86] proposed two phenomenological models namely: the exohedral electric double-sphere supercapacitors model for spherical electrodes and the exohedral electric double-cylinder supercapacitors model for cylindrical electrodes in order to rationalize the relation of capacitance and the size of the OLC or CNT. The origin of the curvature effects that the EDL capacitance increases as the size of spherical/cylindrical electrodes decreases displayed by both theoretical models is yet to be fully understood. Many efforts have been made to demonstrate that there are different C–V curves observed and predicted for planar supercapacitors (e.g., the U-shaped, bell-shaped, and camel-shaped ones) [83,96–100]. However, few studies have concentrated on how the differential capacitance varies with applied potentials for exohedral supercapacitors with OLC/CNT-based electrodes and RTIL electrolytes.

RTIL-based supercapacitors ability to work under a quite wide temperature range broadens the application of supercapacitors under severe conditions due to its excellent thermal stability [84,102,103]. A number of research groups have explored the temperature influence on the capacitance of supercapacitors with RTIL electrolytes. Theoretical and experimental work showed that the capacitance increases with temperature [85,86], a negative temperature dependence (i.e., the capacitance decreases with an increase in temperature) [83,88], and even a complex (e.g., bell-

shaped) capacitance-temperature relationship. Lin et al. [84] reported recently that OLC based supercapacitors with RTIL electrolytes exhibited a positive temperature-dependent capacitance, while that of a vertically aligned CNT electrodes was almost independent of the temperature. MD simulations were performed to model RTIL-based supercapacitors with OLC/CNT electrodes as a function of temperature in order to gain molecular insights into the temperature dependence of capacitance [101,103].

A Monte Carlos MC study showed that a change in ion packing and the location of the counter-ions on the charged surface in particular plays a big role in the temperature dependency of the double-layer capacitance near a charged pore wall [89].

MD simulations constitute a unique tool to provide detailed molecular insights into the capacitive behaviour of RTIL-based supercapacitors with different types of carbon electrodes. The capacitance of porous supercapacitors was found to correlate closely with the specific nature of RTILs the generic features of pores and the applied potential.

In addition to the development of supercapacitors with enhanced energy density, improving the power handling (the charging/discharging process) is another important aspect of supercapacitors [104] which is influenced largely by electrolyte transport associated with ion diffusion. Although numerous studies have been carried out on the properties of supercapacitors in equilibrated status, little efforts have been made to investigate the dynamic process of charging/discharging of a supercapacitors using modelling.

In the absence of a solvent and having a more complex molecular structure, the classical description of EDL formation completely breaks down for RTILs, thus an acute need for advanced theoretical modelling and experimental work. MD simulation can help greatly to develop design strategies for supercapacitors electrodes and selection criteria for the optimized size of SWCNTs since the dependency of the differential capacitance of CNT-based supercapacitors on the potential remains unclear until now.

It is well known that the temperature has an important impact on the performance of supercapacitors devices beside the influence of electrode curvature. Majority of experimental studies observed an increased capacitance with a temperature increase [82,85,86] while some other work reported the exact opposite effect – negative temperature dependence [83].

Interestingly, most theoretical and modelling studies predict the negative temperature dependence or, at least, a complex capacitance-temperature relationship [87–90]; for example, MD simulations by Vatamanu et al. [88] revealed a decrease of capacitance with an increase of temperature, and Monte Carlo simulations by Boda and Henderson, [90] showed a bell-shaped trend delineating the dependence of capacitance on temperature.

Recent experiment using vertically aligned CNT electrodes and RTIL electrolytes revealed that the capacitance was almost independent of the temperature [84]. Hence, an in-depth investigation is needed to establish a reasonable understanding of the temperature dependency as well as the fundamental mechanisms behind this interesting phenomenon.

Guang Feng et al. [101] observed that the capacitance of EDL near the CNT electrode is nearly independent of the temperature, at least within the range between 260 and 400 K, which computationally reproduces the novel experimental findings by Lin et al. [84] for the first time.

However, they noted that the actual device performance regarding the power rating and charge/discharge rates which greatly depend on ion mobility rather than ion packing cannot be predicted from the temperature independence of capacitance.

Comparatively, dynamic effects have been modelled to a lesser extent and suggestions for exploiting these effects to increase EDLs

performance are lacking. Future work in molecular modelling could expand to include a greater focus on ionic transport and charging–discharging kinetics to characterise, and improve performance of dense RTIL electrolytes in nanoporous carbons. Again, simulations that predict kinetics under different charging–discharging rates will be useful for optimisation of energy and power densities. Dynamic EDLS phenomena have so far only been modelled to study polarisation relaxation, temperature, electrode geometry, and ion size effects. Addition of an organic solvent to RTILs could lead to increased electrolyte performance, however molecular modelling has shown the capacitance behaviour to be complex. The addition of an organic solvent can reduce viscosity and ESR and as well increase ionic conductivity, and relative permittivity.

However, this is compensated by a reduction in ionic density due to solvent molecules electrostatically screening interactions and reducing ionic correlations, which in turn lowers the capacitance.

Simulations of more complex electrode structures, such as three-dimensional hierarchical porous networks, are noticeably lacking and their inclusion in molecular models would provide a higher degree of realism and may offer new avenues to further improve EDLS performance. Similarly, pseudocapacitors and battery-EDLC hybrids are both areas of research that are receiving significant attention experimentally. However, accurate models for these systems are currently limited to a few MD simulations [131,132] and ab initio calculations [133–137]. Developing effective models in these areas may be crucial for efficiently identifying conditions and materials that can lead to huge gains in EDLC performance.

## 2.5. Quantum models (*ab initio* quantum chemistry and DFT)

The Car-Pirandello approach based on the electron density functional theory (DFT) [52] is one of appropriate methods for solving problems with the use of *ab initio* molecular dynamics; it allows the consistent investigation of the properties of the ionic sub-system of the electrolyte and electron-hole subsystem of the electrode in a single calculation.

The density functional theory is based on the assumption that the energy of the electronic subsystem is a functional of the electron density  $E^{KS}[n(r)]$  and that the energy of the ground state ( $T = 0$ ) corresponds to the minimum of this functional.

Lankin et al. [47] constructed a quantum mechanical model based on the density functional theory, which made it possible to describe the properties of the electrolyte and electron-hole subsystem of the solid electrode, as well as the electrical double layer at the interface between the electrolyte and carbon material.

Recent attention of theoretical and simulation work on ionic liquids appears to be justified, following their unique characteristics as an electrolyte with low vapour pressure, versatile chemical functionalities, and wide electrochemical potential windows. Enormous efforts have been channelled towards the investigation the ionic liquid electrolyte capacitance dependence on the pore size in the subnanometer region. Kornyshev and co-workers [91] explained the anomalous increase as image forces exponentially screening out the repulsion of the same-charged counterions inside of the narrow pore phenomenological model of charged ions inside of a metallic slit pore.

De-en and Jianzhong [95] addressed the issue of microscopic behaviour of the electrode/electrolyte interface and the capacitance dependence on the pore size with the classical density functional theory (CDFT). Although CDFT had been extensively used to study the EDL structure in aqueous systems, it was not used to investigate the differential capacitance at the electrode/non-aqueous

electrolyte interface as well as the pore size dependence of an EDLC. De-en and Jianzhong realized the great potential of the CDFT method in offering a microscopic view with minimal molecular details and computational cost, and also its ability to address a large pore size range from that comparable to the ionic size to macroscopic scales. To integrate a polar solvent into the CDFT calculations in order to test the desolvation hypothesis and discover the contrast between ionic liquids and organic electrolytes is straightforward.

Basic ideas and applications of CDFT to electrolyte systems have been discussed in recent reviews [108,109] and it pointed out that mathematical foundation of CDFT is the same as that of the well-known electronic DFT [110]. CDFT for electrolytes expresses the free energy as a function of the local densities of ions and solvent molecules instead of presenting the system energy as a function of the electronic density.

The simplicity of this theoretical model also enhances the observation of physical origin of the capacitance oscillation in an ionic liquid electrolyte and also full understanding of key parameters over a wide range of conditions. CDFT predicts strong oscillation of the ionic density profiles near a charged surface [111,112], and a small separation between two charged surfaces leads to the interference of the ionic density profiles in the corresponding EDLs. Having a more realistic model for the ionic liquid, CDFT is expected to be able to predict more complex shapes of the capacitance-potential curves and their respective charging mechanisms as well as the change of the curvature from the bell shape to the u-shaped with the pore size [107].

A complete picture of capacitance as the pore varies from the subnanometer range to mesoscopic scales ( $>2$  nm) is provided by the CDFT simulations. Capacitance virtually becomes independent of pore size when the pore size is larger than a few nanometres. Modelling of EDLSs behaviour in the past relied on a division of the pore size range into several regions, such as below 1, 1–2, and 2–5 nm, etc. [105,106], which becomes irrelevant as it provides a continuous variation of EDL structure and capacitance as pore size changes when CDFT is applied. Good agreement with experiments reflects a fact that CDFT captures the most important physics in the ionic system.

Factors that could further enhance the understanding of organic electrolyte EDLSs such as size of solvent molecules, solvent polarity, ionic concentrations, ionic charges, size disparity between cations and anions, and the shape of the electrode (for example, slit versus cylindrical versus spherical [113] versus ink-bottle pores [114]) remained unanswered questions for CDFT investigations. It would also be interesting to look into the effects of those factors on the comparison between the integral capacitance and the differential capacitance [115].

The CDFT approach could address a modelling challenge of how to establish a predictive structure-capacitance relationship for a real porous material and specific electrolytes. The CDFT approach [116,117] represents the state-of-the-art method used by experimentalists to characterize the surface area and the pore size distribution of porous materials. One can in principle, predict the capacitance of realistic porous electrodes by combining the pore size distribution with the capacitance against pore size relationship from CDFT. Consequently, CDFT modelling can cover the complete process of energy storage in EDLSs, from porosity characterization to EDL structures, capacitance estimation, and charging kinetics. There is still a long way to go for the CDFT to fully incorporate the complexity of the porous electrodes and predict the best electrolyte and porous architecture to maximize the energy and power densities of practical EDLSs. A great challenge from a modelling perspective remains how to establish a predictive structure capacitance relationship for a real porous material and specific electrolytes.

## 2.6. Simplified analytical models

The last type of model is developed on the basis of the EDLS's underlying physics. A set of mathematical equations is used to describe the physical phenomena that govern the properties of the device such as the transport of charged species and the electrochemical reaction rate at the interface [19,21,53–56]. The ESs is classified into two types based on the main physical phenomenon that contributes to the overall capacitance of the device: electric double-layer capacitance implying no charge transfer across the interface and pseudocapacitance (a fast and highly reversible electrochemical reaction that leads to an additional contribution of double-layer charge at the interface). This additional charge depends exponentially on the potential difference appearing across the electrode interfacial double layer. The ESs models are commonly developed with an underlying assumption that the system has a constant interfacial capacitance, a constant concentration of species and physicochemical parameters throughout the electrolyte, and the electrolytes are binary (binary salt and solvent) while the electrochemical reactions are neglected. With such assumptions, different aspects of ESs were studied, including the impact of side reactions [53], porous electrode structure [54,55], and the prediction of specific energy and specific power [56]. Karthik et al. [16] developed a reduced models for an electrochemical supercapacitor analysed with scaling arguments, calibrated and validated with experimental data without accounting for equation of change for energy and heat generation by assuming temperature effect and side reactions to be negligible and an isothermal condition for the system.

The key advantage of the simplified analytical model is its ability to characterize the electrical behaviour of the ESs by means of the partial differential equations that describe the physical phenomena inside the device. This approach provides a lower level of empiricism and is more flexible in including additional parameters and sets of equations. However, this model cannot be used to predict the aging process (pointed out by Doyle et al. [56] in their paper on battery models, which share a similar modelling methodology with the analytical ES models). This is mainly due to the missing features of the analytical models such as the omission of thermal coupling variables and the non-homogeneity of the electrolyte near the interface. Kazaryan et al. [17] developed models for the calculations, control, and improvement of the energy, capacity, power, and other parameters important for safe and long operation of various types and designs of EDL heterogeneous electrochemical supercapacitors (asymmetric) with simultaneous account of physical, electrical, electrochemical properties of electrode materials, designs, and spatial structures of electrodes and separator. They assumed that the negative electrode does not have self-discharge; the potential of the positive electrode being non-polarizable does not change during the charge/discharge and does not depend on the coordinates in the range of the positive electrode.

Jin et al. [57] developed model for a simple planar electrochemical capacitor and from where they showed that the nonlinear polarization density and electrolyte solution should not be neglected. Also they noticed that the modelling of the interfacial region is of important interest because majority of the energy is stored in this very small region that behaves dynamically as a function of many variables, such as electric and thermal fields, local concentrations of species and impurities. Julian et al. [35] developed three-dimensional model for ESs with mesoporous electrodes consisting of cylindrical pores and were used to investigate the effects of (i) pore radius, (ii) electrolyte field-dependent permittivity, (iii) porosity, (iv) effective ions diameter, and (v) electrolyte properties on diffuse layer gravimetric capacitance of the ESs. They established that reduction of ion effective diameter and pore radius

resulted in strongest increase in diffuse layer gravimetric capacitance.

Ganesh M and Sanjeev K. G [58] derived from first principles of ionic movement one-dimensional 1D and two-dimensional 2D models of electrochemical supercapacitor with no faradic reaction using isotropic transport properties to explain a recovery of potential during relaxation after discharge/charge and its dependence on current and concentration, and failure of the ES during charging at high currents and low concentrations of electrolyte.

Conductivity of polarizable electrode during charging and discharging may change in a wide range subject to the specific capacitance parameters, type of conductivity, and the electro-physical parameters of the polarizable electrode. This change has considerable effect on both the capacitance and other parameters of electrochemical supercapacitors. The parameter changes must be put into considerations in order to obtain more precise results. Fig. 7 shows the distribution of electric charge and potentials in the walls of pores and in the electrolyte inside the pores of negative carbon electrode with p-type conductivity. Change of the conductivity types that result in emergence of physical p-n transition occurs in the near-surface layer of walls of the pores in electrode during strong polarization. The thickness and distribution of volume spatial charge of p-n transition depends on the electrophysical parameters of solid electrode material, electrolyte, and potential of the electrode.

Polarizable electrodes of electrochemical supercapacitors are in general, degenerate semiconductors of p-type conductivity in which the Fermi level ( $E_F$ ) is in the valence band. The surface layers of wall pores play an extremely important role in EDL parameters when there is strong polarization of these electrodes. when there is a strong bend of the bands in the near-surface layers of the wall pores by  $\delta$  thickness, Fermi level  $E_F$  is above the conductivity band bottom (material in this area is a degenerate material with p-type conductivity) as could be seen in Fig. 7. Numerous nonlinear effects should be expected both in the near-surface layers of the walls and in wall pores subject to anisotropy of electrode materials as well as different dimensions and forms of the pores. The capacitance of EDL from side of the electrolyte and from side of the solid body (electrode) are serially connected with each other, and parameters of wall pores [118] play a major role in the change of EDL total capacitance.

Kazaryan et al. [17] developed an analytical model of asymmetric supercapacitors that made it possible to calculate energy, capacity, power parameters, energy efficiency of charge-discharge cycles of the capacitors subject to type and value of conductivity of solid matrixes of electrodes with EDL, conductivity of electrolyte, thickness and specific capacitance of electrodes, and values of charge and discharge currents of the capacitors.

They also observed that the growth of the specific (by volume) capacitance of the polarizable electrode results in an increase in specific energy parameters of the capacitors and the growth of polarization and depolarization energy losses which comes as heat. The major portion of energy losses resulted from polarization resistance of the electrodes and electrolyte while some portion is due to depolarization of the potentials of the electrodes. Also, they noticed that energy efficiency of charge-discharge cycles of supercapacitors depends significantly on conductivity of electrode with EDL and the electrolyte, thickness of electrode, and value of charge-discharge currents. An increase in the conductivity of the solid matrix of the electrode and the electrolyte decreases nonlinearly the polarization and depolarization losses of energy during the charge and discharge of supercapacitors.

While several mathematical models for symmetric supercapacitors have been developed, John A. Staser and John W. Weidner also developed a generic hybrid asymmetric

supercapacitor composed of a positive redox couple electrode and a negative double-layer electrode and possess higher energy and power density than the symmetric supercapacitor [138]. The high rate of charge transfer in redox couple electrodes leads to high power density while a negligible mass (because the redox electrode is very thin) leads to high energy density hence the supercapacitors high energy and power densities.

### 3. Heat generation and thermal modelling of ESs

Electrochemical supercapacitors are charged and discharged at very high current rate and this operating mode generates huge amount of heat inside the supercapacitor cell. The equivalent series resistance (ESR) is decreasing, while the capacitance and the self-discharge are increasing with an increase temperature [59–62].

ECs encounter “self-heating” when in use, which is accelerated as the interfacial electric field (related to voltage across the device) and temperature (related to self-heating/internal power dissipated that can be correlated with the current profile) increase. The process of heating-up itself raises the temperature of the device by promoting irreversible side reactions which decrease the ionic conductivity of the electrolyte. The decrease in the ionic conductivity, assuming all other things remain equal, results in additional heat generation which over time leads to thermal runaway.

During EDLS charging and discharging, a portion of the electrical energy is lost as heat. The heat generation rate is dependent on the cell design, its materials, and its operating conditions [120]. Elevated temperatures results in the following: accelerated aging of the supercapacitors [109–124], increased self-discharge rates [119,121–123], increased cell pressure, and possibly electrolyte evaporation [123]. The resistance of supercapacitors increases and its capacitance decreases as it age, which this in turn leads to higher cell temperature and voltage [124]. Temperature differences between series-connected EDLSs can also cause voltage imbalances and destructive overvoltage of individual cells [119,120]. Thermal modelling can be used to predict operating temperatures and develop thermal management strategies for existing EDLS designs, and also to predict the thermal behaviour of novel EDLS designs.

The lifetime expectancy and performance of ES is reduced in an irreversible way due to heat generated by losses from the carbon and conductor electronic resistance and from the electrolyte ionic resistance. The temperature inside supercapacitors varies as a function of the position and the time. For electrical conductors, a large number of free electrons move and transport electric charges, and as such carries thermal energy from high temperature region to low-temperature region. The thermal diffusion is related to internal geometry of the supercapacitor and operating conditions. The temperature at any point in the supercapacitor depends on three modes of heat transfer: conduction, convection, and radiation. Parasitic electrochemical reactions of electrolyte, such as oxidation, are accelerated at higher temperatures, according to Arrhenius law, and similarly at increased voltages. As a result of this continuous process, the capacitance decreases while internal resistance and self-discharge rate rises. Due to the strong dependency on temperature, it is necessary to know the thermal behaviour of EDL supercapacitors.

A thermal simulation model remains a valuable tool for the design of future cells as well as its cooling strategies. It is therefore of great importance to get a mathematical representation of the heat generation mechanisms.

Electrothermal behaviour of supercapacitors can be difficult to predict because a large series of transport phenomena (ionic and electronic transport, heat and mass diffusion) and structure heterogeneities are involved. Temperature profiles depend upon the internally generated power losses which could be non-uniform within electrochemical cells.

The relation between heat production rate during continuous charge-discharge and temperature  $T(M, t)$  at any point in electrochemical supercapacitor cell is basically governed by the heat diffusion expression:

$$\nabla \cdot (-\lambda(M) \cdot \nabla T(M, t)) + C_p \frac{\partial T(M, t)}{\partial t} = Q_V \quad (16)$$

The heat generation rate  $Q_V$  is caused by the following:

- Ionic transport in electrolyte (electrodes and separator) and electronic charge transport in current collectors and solid matrix of electrodes.
- Reversible–irreversible electrochemical reactions at solid-liquid interface of the porous structures.
- Thermal contact and electrical resistances between its layers.

Guillemet et al. [61] using their model performed thermal analysis on supercapacitors, from where they pointed out that maximum temperature is reached at the centre of the cell association as expected.

Anna d'Entremont and Laurent Pilon [125] developed physical modelling and understanding of the coupled electrodiffusion, heat generation, and thermal transport occurring in electric double layer supercapacitors during constant current charge/discharge cycles operation. Their model is important because it predicts both the spatial and temporal variations of the different heat generation rates and the temperature inside EDLSs from first principles and accounted for the irreversible Joule heating as well as three reversible heat generation rates due to ion diffusion, steric effects, and changes in entropy of mixing. The reversible heat generation rates are exothermic during charging, endothermic during discharging, and localized in the EDLs. They were able to reproduce experimental data previously reported in the literature, providing some verification to their model.

The temperature evolution they predicted were remarkably similar to that observed experimentally by Guillemet et al. [61] and Gualous et al. [126] which indicates that the physical model captured the physical phenomena governing the thermal behaviour of EDLCs.

Odne et al. [127] observed from experimental results that a lower thermal conductivity for OLC materials for dry and wet electrodes strongly implied that a high net pore volume is detrimental to conduction of heat, and needs to be taken into account while designing electrodes from materials with a very high pore volume or low packing density.

Modelling supercapacitors internal temperature profiles under conditions corresponding to extreme cycling and a commercially sized unit demonstrated that temperature gradient of several degrees dependent on the ohmic resistance of the cell and on the wetting of the electrode materials are expected.

### 4. Charge redistribution and self-discharge of ESs

The challenge of supercapacitors self-discharge is yet to be thoroughly summarized in review articles up till date and this is important since Electrochemical Supercapacitors are energy storage devices characterized by fast self-discharge process [24,63–80]. Factors influencing the amount of energy stored at certain temperatures [72,75] and the manner of initial charging or charging history [71] have been investigated. To aid in identification of ES electrode self-discharge mechanism, Conway et al. [64,74] proposed mathematical models which predict the self-discharge profile based on three possible mechanisms of self-discharge.

A major obstacle for application of ESs is the charge and energy losses due to self-discharge. Recently, this issue has been investigated by number of laboratories [52,66,69,70,73]. Ricketts and Ton-That [67] came to the conclusion that self-discharge consists of relatively fast diffusion process and a slower leakage current. Open circuit voltage decay as a result of charge losses could be caused by side reactions which may be due to over-potential decomposition of the electrolyte, redox-reactions caused by impurities or possible functional groups on electrodes surface. Also observed self-discharge is due to flaws during supercapacitors production which may result in micro-short circuits between the anode and the cathode [9].

Maximilian et al. [81] from their experiments and models clearly showed that majority of the noticed voltage decay is not caused by real self-discharge since self-discharge is attributed to processes where charge carriers go into side reactions and are not available any more for discharging. In the case of the EDLSs, this accounts only for a very small rate. This observed voltage decay is mainly due to the redistribution of the charge carriers which can be discharged from the device with sufficient discharge time. These findings, from technical point are of great relevance for application where no recharging occurs for long periods of time and where the remaining energy is needed e.g. for cracking an engine. A well charged cell only shows very slow loss of voltage and power.

## 5. Modelling challenges

Simple charge-discharge cycle of an ES demands enough knowledge regarding the impact of the following: 1) the device geometry on device characteristics, 2) electronic and ionic contributions on electric potential, and 3) temperature and interfacial electric field on interfacial chemical reactions. The process of modelling a supercapacitors system involves modelling of the porous separator soaked in electrolyte, the interfacial regions between porous electrodes and electrolyte, the bulk electrode, and metallic contacts between electrode and current collector. Each stage/layer needs to be modelled differently (i.e., pores should be treated as a heterogeneous structure but the kinetics in the bulk and interface differ significantly) and also the interface between the porous electrode and electrolyte. The electric field in the interfacial region together with the temperature field determines the kinetics within the supercapacitors. It is necessary to start with a simple system first and then increase the models complexity in stages in order to analyse and characterize such a complex device.

Development of a large-signal time-dependent model that assumes a constant temperature (implies injecting current for a short time to avoid self-heating) which is a necessary step since it allows the physics of the interfacial region at constant temperature to be validated first is the first stage.

Also, the process of thermal runaway is the key element missing in all of the existing supercapacitors models. The approaches of all the models neglected this runaway process and also through oversimplifications limit further inclusion of coupling variables. The models cannot be used to study the effect of the cell design and operation of on the heat generation during constant-current cycling and so is difficult to develop a thermal-management strategy for the electrical systems in order to maintain the operating temperature and the temperature uniformity of the supercapacitors within a suitable range. Models which relaxes the assumptions made in the existing analytical models by characterizing the electrolyte solutions using all the constituting species, heat generations, charge redistribution effects, self-discharge effects, polarization and depolarization losses of energy as well as taking due account of the supercapacitor component's key parameters and other factors in a rigorous manner is required. The

model will capture the physical and electrochemical phenomena by considering conservation of charge, species and energy along with relevant constitutive relations for the electric double-layer charging and faradic reaction. It has to do the same thing for all the layers and groups within the cell at macro and micro scales.

However, a charge and discharge cycle of electrochemical supercapacitors demands the knowledge concerning the effect of the capacitor geometry, electronic and ionic contributions to electric potential and interfacial chemical reactions as a function of interfacial electric field and the temperature.

## 6. Conclusions

Modelling and simulation remains a key to success in designing tomorrow's high-energy and high-power cells, and as such mathematical theory that moves beyond equivalent circuits to coupling charging to mechanics, energy dissipation, and use of physics and chemistry of solvents and ions in nanoporous electrode materials as well as the electronic and ionic transports in supercapacitor electrodes is required. It is therefore of utmost need to develop from first principles of physics and electrochemistry the needed mathematical model and theoretical basis for design, optimization and fabrication of the desired high-energy and power density, high energy efficiency and long lifecycle subject to more realistic assumptions.

The ESs are to be modelled subject to: (i) electronic, atomic, and molecular polarization of the solvent; (ii) deformation of external electron shells of ions and molecules of the electrolyte in EDLS, (iii) changes of conductivity and density of electron levels on the surface of the solid matrix of the electrode subject to the potential; and (iv) formation of the volume spatial charge in the near-surface layers of the electrode's solid matrix; (v) a strong dependence of the capacitance of the polarizable electrodes on their potential so as to increase the accuracy of theoretical calculations of the parameters and interpretation of the experimental results of different capacitors in a wide range of operating voltages.

The increase of the density of the quasi-free electrons (holes) and ions in the volume of the spatial charge of the electrode and electrolyte, respectively, during the capacitors' charge results to strong interactions that make the value of the ES capacitance to become a function of its electric charge, properties of the electrolyte, and solid electrode materials. Therefore, Equation (1) makes it possible to evaluate only the maximum expected value of EDL supercapacitance, and in order to obtain a more precise value of the capacitance it is appropriate to take account of its electric charge, properties of the electrolyte, and solid electrode material in Equation (1) above.

Although, the investigation of the temperature effects on the performance of IL-based supercapacitors with surface-curved electrodes performed by Guang Feng et al. [101] revealed that the capacitance of the CNT-based supercapacitors is nearly independent of the temperature due to little variation in the EDL structure, and the capacitance of OLC-based increases with temperature due to the decrease of EDL thickness with increasing temperature which computationally reproduces the novel experimental findings by Lin et al. [84]; they also noted that the actual device performance regarding the power rating and charge/discharge rates which greatly depend on ion mobility instead of ion packing cannot be predicted from the temperature independence of capacitance.

The mechanism at the origin of the enhanced capacitance in nanoporous electrodes can be fully understood from molecular dynamics simulations involving realistic carbon materials and taking into consideration the polarization effects in an appropriate way [128], since it is the correct introduction of polarization effects by metallic walls could allow for a complete understanding of the formation of a superionic state [91,92].

Moreover, the lifetime expectancy and performance of EDLS is reduced in an irreversible way due to heat generated by polarization and depolarization energy losses, carbon and conductor electronic resistance and the electrolyte ionic resistance. This process of self-heating raises the temperature of the device and promotes irreversible side reactions which decrease the ionic conductivity of the electrolyte and assuming all other things remain equal, results to additional heat generation which over time leads to thermal runaway.

Thermal model is very important because it predicts both the spatial and temporal variations of the different heat generation rates and the temperature inside EDLSs from first principles and account for the irreversible Joule heating as well as three reversible heat generation rates due to ion diffusion, steric effects, and changes in entropy of mixing.

Therefore, models incorporating a thermal model will present the needed internal temperature distribution profile that will aid in designing electrodes materials, predicting operating temperatures and developing thermal management/cooling strategies for existing and novel EDLS cell designs as well as their operating conditions. The coupled model will provide the needed temperature distribution of the supercapacitors, which could be utilized in the determination of the optimum loading for the device without losing ions through irreversible chemical reactions or gas formation in the electrolyte.

Simulations of more complex electrode structures, such as three-dimensional hierarchical porous networks, are noticeably lacking and their inclusion in molecular models would provide a higher degree of realism and may offer new avenues to further improve EDLS performance. Similarly, pseudocapacitors and battery-EDLC hybrids are both areas of research that are receiving significant attention experimentally.

The future efforts and proposed model for improving the performance and life-time of the electrochemical supercapacitors demands a more detailed model of the supercapacitors that is based on large signal formulation that couples the thermal and electric fields and also subject to the type and value of conductivity of the electrodes, thickness, porosity and specific capacitance of electrodes, conductivity of electrolyte, thickness and porosity of separator and the values of charge and discharge currents.

## Acknowledgements

The support of the Department of Science and Technology/National Research Foundation, DST/NRF Centre of Excellence in Strong Materials (CoE-SM) and the School of Chemical Metallurgical Engineering, University of the Witwatersrand, Johannesburg, South Africa towards this research is hereby acknowledged. Opinions expressed and conclusions arrived at, are those of the authors and are not necessarily to be attributed to the CoE-SM.

## References

- [1] D. Pech, M. Brunet, H. Durou, P. Huang, V. Mochalin, Y. Gogotsi, P.L. Taberna, P. Simon, *Nat. Nanotechnol.* 5 (9) (2010) 651–654.
- [2] A.G. Pandolfo, A.F. Hollenkamp, *J. Power Sources* 157 (1) (2006) 11–27.
- [3] E. Frackowiak, *Phys. Chem. Chem. Phys.* 9 (15) (2007) 1774–1785.
- [4] P. Simon, Y. Gogotsi, *Nat. Mater.* 7 (11) (2008) 845–854.
- [5] L.L. Zhang, X.S. Zhao, *Chem. Soc. Rev.* 38 (9) (2009) 2520–2531.
- [6] Shuai Ban, Jiuju Zhang, Lei Zhang, Ken Tsay, Datong Song, Xinfu Zou, *Electrochim. Acta* 90 (2013) 542–549.
- [7] Dorin Petreus, Daniel Moga, Ramona Galatius, Radu A. Munteanu, *Adv. Electr. Comput. Eng.* 8 (2) (2008), <http://dx.doi.org/10.4316/AECE.2008.02003>.
- [8] S. Bose, T. Kuila, A.K. Mishra, R. Rajasekar, N.H. Kim, J.H. Lee, *J. Mater. Chem.* 22 (2012) 767–784.
- [9] B.E. Conway, *Electrochemical Supercapacitors: Scientific Fundamentals and Technological Applications*, Plenum Pub Corp, 1999, p. 222.
- [10] H. Jiang, J. Ma, C.Z. Li, *Adv. Mater.* 24 (2012) 4197–4202.
- [11] C.D. Lokhande, D.P. Dubal, O.S. Joo, *Curr. Appl. Phys.* 11 (2011) 255–270.
- [12] M.D. Stoller, R.S. Ruoff, *Energy Environ. Sci.* 3 (2010) 1294–1301.
- [13] R.P. Richner, *Entwicklung neuartig gebundener Kohlenstoff- materialien für elektrische Dop-pelschichtkondensatorelektronen* (PhD thesis), Swiss Federal Institute of Technology Zurich, 2001, p. 176.
- [14] Manisha Vangari, Tonya Pryor, Li Jiang, *J. Energy Eng.* 139 (2) (2013) 72–79.
- [15] M.W. Verbrugge, P. Liub, *J. Electrochem. Soc.* 152 (5) (2005) D79–D87.
- [16] Karthik Somasundaram, Erik Birgersson, Arun Sadashiv Mujumdar, *J. Electrochem. Soc.* 158 (11) (2011) A1220–A1230.
- [17] S.A. Kazaryan, S.N. Razumov, S.V. Litvinenko, G.G. Kharisov, V.I. Kogan, *J. Electrochem. Soc.* 153 (9) (2006) A1655–A1671.
- [18] S. Vazquez, S.M. Lukic, E. Galvan, L.G. Franquelo, J.M. Carrasco, *IEEE Trans. Ind. Electron.* 57 (12) (Dec. 2010) 3881–3895.
- [19] S. Devan, V.R. Subramanian, R.E. White, *J. Electrochem. Soc.* 151 (6) (2004) A905–A913.
- [20] H. Kim, B.N. Popov, R.E. White, *J. Electrochem. Soc.* 150 (9) (2003) A1153–A1160.
- [21] C. Lin, B.N. Popov, H.J. Ploehn, *J. Electrochem. Soc.* 149 (2) (2002) A167–A175.
- [22] F. Belchambi, S. Rael, B. Davat, in: *Proc. Conf. Record IEEE Ind. Appl. Soc.*, vol. 5, 2000, pp. 3069–3076. Rome, Italy.
- [23] F. Rafik, H. Gualous, R. Gallay, A. Causaz, A. Berthon, *J. Power Sources* 165 (2) (2007) 928–934.
- [24] Y. Diab, P. Venet, H. Gualous, G. Rojat, *IEEE Trans. Power Electron.* 24 (2) (Feb. 2009) 510–517.
- [25] R. de Levie, *Electrochim. Acta* 8 (1963) 751–780.
- [26] D.B. Robinson, *J. Power Sources* 195 (2009) 3748–3756.
- [27] J. Black, H.A. Andreas, *J. Power Sources* 195 (2009) 929–935.
- [28] E.H. El Brouji, O. Briat, J.M. Vinassa, N. Bertrand, E. Woigard, *IEEE Trans. Veh. Technol.* 58 (8) (Oct. 2009) 3917–3929.
- [29] R.J. Hunter, *Foundations of Colloid Science*, vol. 1, Clarendon, Oxford, 1987.
- [30] G. Gouy, *J. Phys. Theor. Appl.* 9 (1910) 457.
- [31] D.L. Chapman, *Philos. Mag. Ser.* 6 (25) (1913) 475.
- [32] J.H. Masliyah, S. Bhattacharjee, *Electrokinetic and Colloid Transport Phenomena*, John Wiley & Sons, Hoboken, NJ, 2006.
- [33] O. Stern, *Z. Elektrochem. Angew. Phys. Chem.* 30 (1924) 508.
- [34] D.C. Grahame, *Chem. Rev.* 41 (1947) 441.
- [35] J. Varghese, H. Wang, L. Pilon, *J. Electrochem. Soc.* 158 (10) (2011) A1106–A1114.
- [36] S.W. Woo, K. Dokko, H. Nakano, K. Kanamura, *J. Mater. Chem.* 18 (14) (2008) 1674–1680.
- [37] Hainan Wang, Laurent Pilon, *J. Power Sources* 221 (2013) 252–260.
- [38] J.B. Freund, *J. Chem. Phys.* 116 (2002) 2194–2200.
- [39] R. Qiao, N.R. Aluru, *J. Chem. Phys.* 118 (2003) 4692–4701.
- [40] A.P. Thompson, *J. Chem. Phys.* 119 (2003) 7503–7511.
- [41] R. Qiao, N.R. Aluru, *Phys. Rev. Lett.* 92 (2004) 198301.
- [42] D. Kim, E. Darve, *Phys. Rev. E* 73 (2006) 051203.
- [43] P. Wu, R. Qiao, *Phys. Fluids* 23 (2011) 072005.
- [44] S.T. Cui, H.D. Cochran, *J. Chem. Phys.* 117 (2002) 5850–5854.
- [45] G. Feng, R. Qiao, J. Huang, B.G. Sumpter, V. Meunier, *ACS Nano* 4 (2010) 2382–2390.
- [46] M.C.F. Wander, K.L. Shuford, *J. Phys. Chem. C* 114 (2010) 20539–20546.
- [47] A.V. Lankin, G.E. Norman, V.V. Stegalov, *High. Temp. ISSN: 0018-151X* 48 (6) (2010) 837–845.
- [48] J. Koryta, J. Dvorak, V. Bohackova, *Elektrochemie*, Academia, Praha, 1975.
- [49] S.A. Kislenko, I.S. Samoylov, R.H. Amirov, *Phys. Chem. Chem. Phys.* 11 (2009) 5584.
- [50] V.V. Chaban, O.N. Kalugin, *J. Mol. Liq.* 145 (2009) 145.
- [51] V.V. Chaban, O.N. Kalugin, *Usp. Khim. Khim. Tekhnol.* 21 (3) (2007) 40.
- [52] B. Pillay, J. Newman, *J. Electrochem. Soc.* 143 (1996) 1806–1814.
- [53] A.M. Johnson, J. Newman, *J. Electrochem. Soc.* 118 (1971) 510–517.
- [54] N. Bertrand, J. Sabatier, O. Briat, J. Vinassa, *IEEE Trans. Ind. Electron.* 57 (12) (Dec. 2010) 3991–4000.
- [55] D. Dunn, J. Newman, *J. Electrochem. Soc.* 147 (2000) 820–830.
- [56] M. Doyle, T.F. Fuller, J. Newman, *J. Electrochem. Soc.* 140 (6) (Jun. 1993) 1526–1533.
- [57] Jin Hyun Chang, Francis P. Dawson, Keryn K. Lian, *IEEE Trans. Power Electron.* 26 (12) (Dec. 2011).
- [58] Ganesh Madabattula, Sanjeev K. Gupta, *Modeling of Supercapacitor*, Excerpt from the Proceedings of the 2012 COMSOL Conference in Bangalore.
- [59] H. Gualous, D. Bouquain, A. Berthon, J.M. Kauffmann, *J. Power Sources* 123 (1) (Sep. 2003) 86–93.
- [60] R. Kötz, M. Hahn, R. Gallay, *J. Power Sources* 154 (2) (Mar. 2006) 550–555.
- [61] P. Guillemet, Y. Scudeler, T. Brouse, *J. Power Sources* 157 (1) (Jun. 2006) 630–640.
- [62] J. Schiffer, D. Linzen, D.U. Sauer, *J. Power Sources* 160 (1) (Sep. 2006) 765–772.
- [63] G. Wang, L. Zhang, J. Zhang, *Chem. Soc. Rev.* 41 (2012) 797.
- [64] B.E. Conway, W.G. Pell, T.C. Liu, *J. Power Sources* 65 (1997) 53.
- [65] W.G. Pell, B.E. Conway, W.A. Adams, J. de Oliveira, *J. Power Sources* 80 (1999) 134.
- [66] B.W. Ricketts, C. Ton-That, *J. Power Sources* 89 (2000) 64.
- [67] J. Niu, B.E. Conway, W.G. Pell, *J. Power Sources* 135 (2004) 332.
- [68] K.M. Kim, J.W. Hur, S.-I. Jung, A.-S. Kang, *Electrochim. Acta* 50 (2004) 863.

[69] S.A. Kazaryan, G.G. Kharisov, S.V. Litvinenko, V.I. Kogan, *J. Electrochem. Soc.* 154 (2007) A751.

[70] S.A. Kazaryan, S.V. Litvinenko, G.G. Kharisov, *J. Electrochem. Soc.* 155 (2008) A464.

[71] J. Black, H.A. Andreas, *Electrochim. Acta* 54 (2009) 3568.

[72] H.A. Andreas, K. Lussier, A.M. Oickle, *J. Power Sources* 187 (2009) 275.

[73] S. Ishimoto, Y. Asakawa, M. Shinya, K. Naoi, *J. Electrochem. Soc.* 156 (2009) A563.

[74] M. Kaus, J. Kowal, D.U. Sauer, *Electrochim. Acta* 55 (2010) 7516.

[75] J. Kowal, E. Avaroglu, F. Chamekh, A. Senfelds, T. Thien, D. Wijaya, D.U. Sauer, *J. Power Sources* 196 (2011) 573.

[76] H. Yang, Y. Zhang, *J. Power Sources* 196 (2011) 8866.

[77] S.H. Kim, W. Choi, K.-B. Lee, S. Choi, *IEEE Trans. Power Electron.* 26 (2011) 3377.

[78] Q. Zhang, J. Rong, D. Ma, B. Wei, *Energy Environ. Sci.* 4 (2011) 2152.

[79] W.G. Pell, B.E. Conway, *J. Electroanal. Chem.* 500 (2001) 121.

[80] B. Xu, F. Wu, Y. Su, G. Cao, S. Chen, Z. Zhou, Y. Yang, *Electrochim. Acta* 53 (2008) 7730.

[81] J. Niu, W.G. Pell, B.E. Conway, *J. Power Sources* 156 (2006) 725–740.

[82] C. Masarapu, H.F. Zeng, K.H. Hung, B. Wei, *ACS Nano* 3 (2009) 2199–2206.

[83] M.T. Alam, M.M. Islam, T. Okajima, T. Ohsaka, *J. Phys. Chem. C* 111 (2007) 18326–18333.

[84] R. Lin, P.-L. Taberna, S. Fantini, V. Presser, C.R. Pérez, F. Malbosc, N.L. Rupesinghe, K.B.K. Teo, Y. Gogotsi, P. Simon, *J. Phys. Chem. Lett.* 2 (2011) 2396–2401.

[85] V. Lockett, R. Sedev, J. Ralston, M. Horne, T. Rodopoulos, *J. Phys. Chem. C* 112 (2008) 7486–7495.

[86] F. Silva, C. Gomes, M. Figueiredo, R. Costa, A. Martins, C.M. Pereira, *J. Electroanal. Chem.* 622 (2008) 153–160.

[87] M. Holovko, V. Kapko, D. Henderson, D. Boda, *Chem. Phys. Lett.* 341 (2001) 363–368.

[88] J. Vatamanu, O. Borodin, G.D. Smith, *J. Am. Chem. Soc.* 132 (2010) 14825–14833.

[89] D. Boda, D. Henderson, K.-Y. Chan, *J. Chem. Phys.* 110 (1999) 5346–5350.

[90] D. Boda, D. Henderson, *J. Chem. Phys.* 112 (2000) 8934–8938.

[91] S. Kondrat, A.A. Kornyshev, *J. Phys. Condens. Matter* 23 (2011) 022201.

[92] S. Kondrat, N. Georgi, M.V. Fedorov, A. Kornyshev, *Phys. Chem. Chem. Phys.* 13 (2011) 11359–11366.

[93] L. Yang, B.H. Fishbine, A. Migliori, L.R. Pratt, *J. Am. Chem. Soc.* 131 (2009) 12373–12376.

[94] Y. Shim, H.J. Kim, *ACS Nano* 4 (2010) 2345–2355.

[95] D.E. Jiang, J. Wu, *J. Phys. Chem. Lett.* 4 (2013) 1260–1267.

[96] A. Kornyshev, *J. Phys. Chem. B* 111 (2007) 5545–5557.

[97] V. Lockett, M. Horne, R. Sedev, T. Rodopoulos, J. Ralston, *Phys. Chem. Chem. Phys.* 12 (2010) 12499–12512.

[98] S. Baldelli, *Acc. Chem. Res.* 41 (2008) 421–431.

[99] M. Trulsson, J. Algotsson, J. Forsman, C.E. Woodward, *J. Phys. Chem. Lett.* 1 (2010) 1191–1195.

[100] G. Feng, J.S. Zhang, R. Qiao, *J. Phys. Chem. C* 113 (2009) 4549–4559.

[101] G. Feng, S. Li, J.S. Atchison, V. Presser, P.T. Cummings, *J. Phys. Chem. C* 117 (2013) 9178–9186.

[102] W.-Y. Tsai, R. Lin, S. Murali, L. Li Zhang, J.K. McDonough, R.S. Ruoff, P.-L. Taberna, Y. Gogotsi, P. Simon, *Nano Energy* 2 (2013) 403–411.

[103] S. Li, G. Feng, P.F. Fulvio, P.C. Hillesheim, C. Liao, S. Dai, P.T. Cummings, *J. Phys. Chem. Lett.* 3 (2012) 2465–2469.

[104] C. Cagle, G. Feng, R. Qiao, J. Huang, B. Sumpter, V. Meunier, *Microfluid. Nanofluid.* 8 (2010) 703–708.

[105] J.S. Huang, B.G. Sumpter, V. Meunier, *Chem. Eur. J.* 14 (2008) 6614–6626.

[106] J.S. Huang, B.G. Sumpter, V. Meunier, *Angew. Chem. Int. Ed.* 47 (2008) 520–524.

[107] L. Xing, J. Vatamanu, O. Borodin, D. Bedrov, *J. Phys. Chem. Lett.* 4 (2013) 132–140.

[108] J.Z. Wu, *AIChE J.* 52 (2006) 1169–1193.

[109] J.Z. Wu, Z.D. Li, *Annu. Rev. Phys. Chem.* 58 (2007) 85–112.

[110] P. Hohenberg, W. Kohn, *Phys. Rev.* 136 (1964) B864–B871.

[111] D.E. Jiang, D. Meng, J.Z. Wu, *Chem. Phys. Lett.* 504 (2011) 153–158.

[112] J.Z. Wu, T. Jiang, D.E. Jiang, Z.H. Jin, D. Henderson, *Soft Matter* 7 (2011) 11222–11231.

[113] G. Feng, D.E. Jiang, P.T. Cummings, *J. Chem. Theory Comput.* 8 (2012) 1058–1063.

[114] P.T.M. Nguyen, C. Fan, D.D. Do, D. Nicholson, *J. Phys. Chem. C* 117 (2013) 5475–5484.

[115] O. Pizio, S. Sokolowski, Z. Sokolowska, *J. Chem. Phys.* 137 (2012) 234705.

[116] P.I. Ravikovitch, A.V. Neimark, *Langmuir* 22 (2006) 11171–11179.

[117] G.Y. Gor, M. Thommes, K.A. Cychosz, A.V. Neimark, *Carbon* 50 (2012) 1583–1590.

[118] R. Kotz, M. Hahn, O. Barbieri, J.-C. Sauter, R. Gallay, in: *The 13th International Seminar on Doublelayer Capacitor and Hybrid Energy Storage Devices*, Dec 8–10, 2003, Deerfield Beach, FL, 2003.

[119] M.B. Camara, H. Gualous, F. Gustin, A. Berthon, B. Dakyo, *IEEE Trans. Ind. Electron.* 2 (57) (2010) 587–597.

[120] W. Henson, *J. Power Sources* 179 (2008) 417–423.

[121] W. Greenwell, A. Vahidi, *IEEE Trans. Ind. Electron.* 6 (57) (2010) 1954–1963.

[122] A. Payman, S. Pierfederici, F. Meibody-Tabar, *IEEE Trans. Power Electron.* 12 (24) (2009) 2681–2691.

[123] S. Lemofouet, A. Rufer, *IEEE Trans. Ind. Electron.* 4 (53) (2006) 1105–1115.

[124] P. Kurzweil, M. Chwistek, *J. Power Sources* 176 (2008) 555–567.

[125] Anna d'Entremont, Laurent Pilon, *J. Power Sources* 246 (2014) 887–898.

[126] H. Gualous, H. Louahlia, R. Gallay, *IEEE Trans. Power Electron.* 26 (11) (2011) 3402–3409.

[127] Odne S. Burheim, Mesut Aslan, Jennifer S. Atchison, Volker Presser, *J. Power Sources* 246 (2014) 160–166.

[128] C. Merlet, B. Rotenberg, P.A. Madden, P.-L. Taberna, P. Simon, Y. Gogotsi, M. Salanne, *Nat. Mater.* 11 (306) (2012).

[129] David B. Robinson, Chung-An Max Wu, Benjamin W. Jacobs, *J. Electrochem. Soc.* 157 (8) (2010) A912–A918.

[130] P. Kurzweil, H.J. Fischle, *J. Power Sources* 127 (2004) 331–340.

[131] J. Vatamanu, O. Borodin, G.D. Smith, *J. Phys. Chem. C* 116 (2011) 1114–1121.

[132] L. Xing, J. Vatamanu, O. Borodin, G.D. Smith, D. Bedrov, *J. Phys. Chem. C* 116 (2012) 23871–23881.

[133] V. Ozolin, F. Zhou, M. Asta, *Acc. Chem. Res.* 46 (2013) 1084–1093.

[134] Y. Liu, F. Zhou, V. Ozolins, *J. Phys. Chem. C* 116 (2011) 1450–1457.

[135] D.A. Tompsett, S.C. Parker, P.G. Bruce, M.S. Islam, *Chem. Mater.* 25 (2013) 536–541.

[136] Z.R. Cormier, H.A. Andreas, P. Zhang, *J. Phys. Chem. C* 115 (2011) 19117–19128.

[137] J. Kang, S.-H. Wei, K. Zhu, Y.-H. Kim, *J. Phys. Chem. C* 115 (2011) 4909–4915.

[138] John A. Staser, John W. Weidner, *J. Electrochem. Soc.* 161 (8) (2014) E3267–E3275.